The Paschen-Back Effect in NH_3 and N_2O Microwave Spectra*

C. K. JEN
Cruft Laboratory, Harvard University, Cambridge, Massachusetts
(Received August 5, 1949)

The Paschen-Back effect in the microwave spectra of NH_3 and N_2O has been investigated in this experiment with a resonant cavity spectroscope. These molecules are known to possess relatively small values of nuclear electric quadrupole coupling and thus favor the realization of the Paschen-Back effect without prohibitively high magnetic fields.

The results for $N^{14}H_3$, representing a case of one-nuclear (N^{14}) coupling, show the effects of gradual decoupling of the nuclear spin from molecular rotation. The existence of the "forbidden" lines, whose intensities diminish with increasing field, indicates that the decoupling is not quite complete even in a field of 10,000 oersteds.

The results for $N^{14}N^{14}O^{16}$, representing a case of two-nuclear (N^{14}, N^{14}) coupling, show that the decoupling is almost complete at a field of 10,000 oersteds. An asymmetry of the Paschen-Back pattern for a $\Delta J \neq 0$ transition is ascribed to the non-linear dependence of the nuclear quadrupole coupling energy upon M_J and M_I.

The measured results are found to be in good agreement with quantum mechanical calculations. Also, consistent with the theory of the structure of the Paschen-Back pattern, it is shown that the molecular g-factors and the nuclear quadrupole coupling factors can be determined directly from experimental data.

I. INTRODUCTION

IN a previous paper,[1] the writer has investigated the Zeeman effect in microwave molecular spectra. It was shown that, if a molecular spectral line possesses a multiplet structure on account of a coupling energy between the nuclear spin and molecular rotation, the Zeeman effect of the multiplet structure can be accounted for by the combined magnetic contributions due to the nuclear and molecular g-factors. The underlying assumption for the Zeeman effect is that the energy change caused by the interaction of the external magnetic field with the nuclear and molecular magnetic moments is very much smaller than the energy differences in the multiplet structure. Under these conditions, the Zeeman splitting is a linear function of the field strength. As the external magnetic field is increased to the extent that the magnetic interaction energy becomes comparable with that of the multiplet separation, significant departures from linearity result. Further increase of the field accentuates still more the role of the magnetic energy relative to the multiplet separation energy, until the field is strong enough to decouple completely the nuclear spin from the molecular rotation. Following the usage in atomic spectra, the phenomenon representing the transition from the state characterized by the Zeeman effect to that of complete decoupling is called the Paschen-Back effect.

The Paschen-Back effect in molecular spectra can play an important role in elucidating the nature of spin-rotation coupling relations in a manner analogous to its role in atomic spectra. It affords a direct means for determining the molecular g-factor, which is responsible for the principal splitting in the completely decoupled state. Also, it gives a further check on the correctness of the theory of the Zeeman effect.

As regards the experimental realization of the Paschen-Back effect, the magnetic field required is essentially determined by the ratio of the spin-rotation coupling to the combined g-factor. It is evident, for any given resolution of the apparatus, that this ratio must be fairly small in order that the requisite magnetic field may not be prohibitively high. In practice, not very many molecules known in microwave spectra can satisfy this condition. The molecules NH_3 and N_2O are fairly typical of those whose electric quadrupole couplings are small enough to make the Paschen-Back effect realizable. They are thus taken as the subject of investigation for the present experiment.

II. A NEW MICROWAVE CAVITY SPECTROSCOPE

The essential features of a microwave resonant cavity spectroscope, together with circuit arrangements and principles of operation, have been presented in (I). For this and subsequent work, however, a new cavity has been constructed which is an integral part of the electromagnet assembly. The new apparatus embodies a number of mechanical improvements for the cavity and an electromagnet supplying a variable magnetic field up to 10,500 oersteds with approximately one percent spatial inhomogeneity.

Figure 1 shows, on the right-hand side, a cylindrical cavity soldered to one end of a magnetic pole piece and, on the left-hand side, a tuning plunger made to slide through another pole piece. The cavity, made of copper, is machined to an internal diameter of 1.949 inches. The hole at the bottom of the cavity is to couple microwave energy into the cavity from a wave guide which passes through the magnetic pole piece. This

* The research reported in this document was made possible through support extended Cruft Laboratory, Harvard University, jointly by the Navy Department, ONR, the Signal Corps of the U. S. Army, and the U. S. Air Force, under ONR Contract N5ori-76, T. O. 1.

[1] C. K. Jen, Phys. Rev. 74, 1396 (1948), hereafter referred to as (I).

coupling hole has a diameter of 0.166 inch and is offset from the center of the cavity by 0.25 inch. The tuning plunger consists of a long beryllium copper rod attached to a copper disk, which, in the assembled position, is able to move axially in the cavity with a very small clearance from the cavity wall. The rear side of the disk (facing the rod) is painted with powdered graphite in a ceramic binder, to attenuate extraneously coupled oscillation modes.

In Fig. 2, the cavity is shown in place between the pole pieces in the assembled position (the cavity being now soldered to the other pole piece as well). A circular loop of insulated wire, for the measurement of the magnetic field strength, is embedded in the wall of the cavity and is connected to an external fluxmeter by a pair of twisted leads. A large mocrometer head, which moves the tuning plunger and the sylphon bellows, controls the cavity tuning. The cavity setting, as measured by the micrometer reading, corresponds to a definite frequency scale for any given mode of oscillation. For very small plunger displacements, corresponding to minute changes in resonance frequency, a demountable precision dial indicator is coupled to the micrometer head, as shown in the picture. Other incidentals such as two pump leads and a mica window at the flange end of the wave guide may also be seen.

Figure 3 gives an over-all view of the whole apparatus when the center section, shown in Fig. 2, is assembled with the rest of the electromagnet. The wave guide leading from the bottom of the magnet indicates the manner of the microwave coupling to other parts of the measuring equipment.

III. EXPERIMENTAL RESULTS FOR $N^{14}H_3$ INVERSION SPECTRUM

The Paschen-Back effect in various $N^{14}H_3$ inversion lines has been found, except for differences in the relative complexity of patterns, to be not fundamentally different from one line to another. As might be expected from its low J-number, the $JK=11$ line shows a simple and more readily resolved pattern. This line is thus an appropriate subject for the present analysis.

Figure 4 shows the frequency separation between the centers of the two branches of σ-components as a function of the field strength. It is seen that a linear relation is maintained up to 3000 or 4000 oersteds. For still higher fields, there is a slight non-linearity and a gradual approach to a new straight line, whose slope corresponds to a g-factor approximately equal to the molecular g-factor (g_{mole}) obtained in (I). The transition is very gradual, as would be expected from the approximate equality between the combined g-factor, which controls the Zeeman splitting, and the molecular g-factor, which controls the Paschen-Back splitting in the decoupled state.

The lower picture in Fig. 5 is a reproduction of the oscilloscopic pattern[2] for the $JK=11$ line at a constant field of 8500 oersteds. The intensities of the strong lines (main π-line at the center and two strong σ-lines on each side of the center) were found to be essentially independent of field, whereas those of the weak lines diminished very noticeably with increasing field. However, the weak lines were found to be still detectable even in a field of 10,000 oersteds.

IV. THEORY OF THE PASCHEN-BACK EFFECT IN MOLECULES WITH ONE-NUCLEAR COUPLING

In order to interpret the experimental results described above, a brief theory of the Paschen-Back effect applicable to a symmetric top or linear molecule with one-nuclear coupling is sketched below. The total Hamiltonian[3] may be written as

$$\mathcal{H}=\mathcal{H}_R+\mathcal{H}_H+\mathcal{H}_Q, \tag{1}$$

where $\mathcal{H}_R$ = Hamiltonian for molecular rotation,

$$\mathcal{H}_H=-g_{\text{mole}}\mu_0\mathbf{J}\cdot\mathbf{H}-g_N\mu_0\mathbf{I}\cdot\mathbf{H},$$
$$\mathcal{H}_Q=C\{3(\mathbf{J}\cdot\mathbf{I})^2+\tfrac{3}{2}\mathbf{J}\cdot\mathbf{I}-\mathbf{J}^2\mathbf{I}^2\}$$

and

$$C=-eQ\frac{\partial^2V}{\partial z^2}\left(1-\frac{3K^2}{J(J+1)}\right)\frac{1}{2I(2I-1)(2J-1)(2J+3)},$$

g_{mole}, g_N = molecular, nuclear g-factors,

$\mathbf{J}$, $\mathbf{I}$ = molecular, nuclear angular momentum vector operators associated with J, I quantum numbers,

K = quantum number for molecular angular momentum along figure axis,

Q = electric quadrupole moment of the nucleus for the state $M_I=I$ (M = magnetic quantum number),

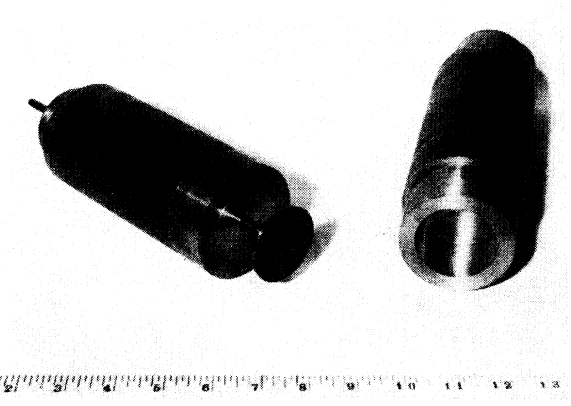

FIG. 1. The microwave cavity and the magnet pole pieces (unassembled view).

[2] A photograph of the entire pattern is not feasible because of the narrow field of the cavity resonance.

[3] The nuclear magnetic dipole interaction with the molecular rotation field is neglected.

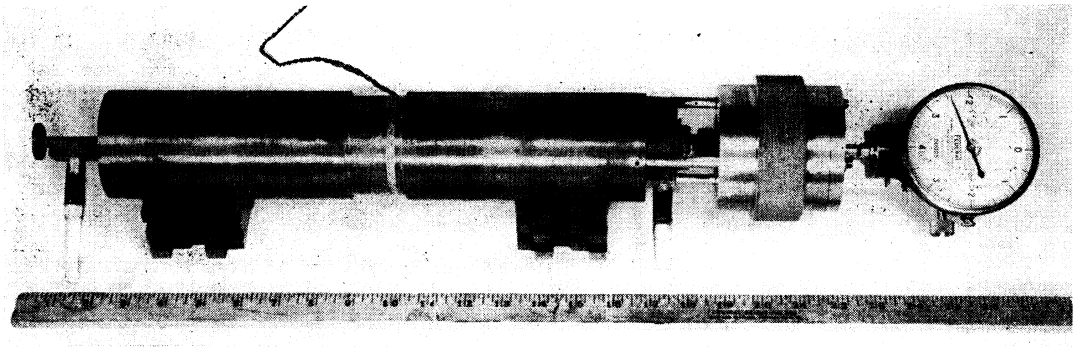

FIG. 2. The microwave cavity and the magnet pole pieces (assembled view).

V = electric potential at the nucleus in question due to all surrounding charges,
z = ordinate along figure axis,
μ_0 = nuclear magneton.

The first term, $\mathcal{H}_R$, on the right-hand side of Eq. (1) represents the Hamiltonian for the rotational state JK (or $JK\delta$, where δ is used for describing inversion or other types of doubling). The second term, $\mathcal{H}_H$, contains the sum of the magnetic energy operators for the molecular and nuclear magnetic interactions. The last term, $\mathcal{H}_Q$, represents the nuclear quadrupole interaction.

In treating the problem for intermediate fields, a representation designated by JIM_JM_I, in which the matrices for $\mathcal{H}_R$ and $\mathcal{H}_H$ are already diagonal (whereas the matrix for $\mathcal{H}_Q$ is not), can be used and then a unitary transformation can be made such that the matrix for $\mathcal{H}$ is diagonal in the transformed representation. The matrix elements for $\mathcal{H}_Q$ are non-vanishing only for the following transitions:

$$\begin{aligned} &\Delta M_J=0, \quad \Delta M_I=0; \\ &\Delta M_J=\pm 1, \quad \Delta M_I=\mp 1; \\ &\Delta M_J=\pm 2, \quad \Delta M_I=\mp 2. \end{aligned} \tag{2}$$

The matrix elements of $\mathcal{H}_H$ and $\mathcal{H}_Q$[4,5] can be shown to be as follows:

$$(M_JM_I|\mathcal{H}_H|M_JM_I)=-(M_Jg_{\text{mole}}+M_Ig_N)\mu_0H, \tag{3}$$

$$(M_JM_I|\mathcal{H}_Q|M_JM_I)=(C/2)\{J(J+1)-3M_J^2\}\times\{I(I+1)-3M_I^2\}, \tag{4}$$

$$\begin{aligned}(M_J\pm 1M_I\mp 1|\mathcal{H}_Q|M_JM_I)&=(3C/4)(2M_J\pm 1)(2M_I\mp 1)\\ &\times[(J\mp M_J)(J\pm M_J+1)(I\pm M_I)(I\mp M_I+1)]^{\frac{1}{2}},\end{aligned} \tag{5}$$

$$\begin{aligned}(M_J\pm 2M_I\mp 2|\mathcal{H}_Q|M_JM_I)&=(3C/4)[(J\mp M_J)(J\mp M_J-1)(J\pm M_J+1)\\ &\times(J\pm M_J+2)(I\pm M_I)(I\pm M_I-1)\\ &\times(I\mp M_I+1)(I\mp M_I+2)]^{\frac{1}{2}}.\end{aligned} \tag{6}$$

The solution for the eigenvalues is obtained by solving the secular equation of the $(2I+1)$th or $(2J+1)$th order (depending on which is smaller). The solution is very simple for an almost infinitely high field (for an assurance of complete decoupling), because only the diagonal elements as shown in Eqs. (3) and (4) need to be considered. The result is

$$\begin{aligned}W(H\to\infty)&=W_R(JK\delta)-(M_Jg_{\text{mole}}+M_Ig_N)\mu_0H\\ &+(C/2)\{J(J+1)-3M_J^2\}\{I(I+1)-3M_I^2\}.\end{aligned} \tag{7}$$

The calculations for the line intensities can be more conveniently carried out by the perturbation method. For brevity, let α denote M_JM_I with J and I as con-

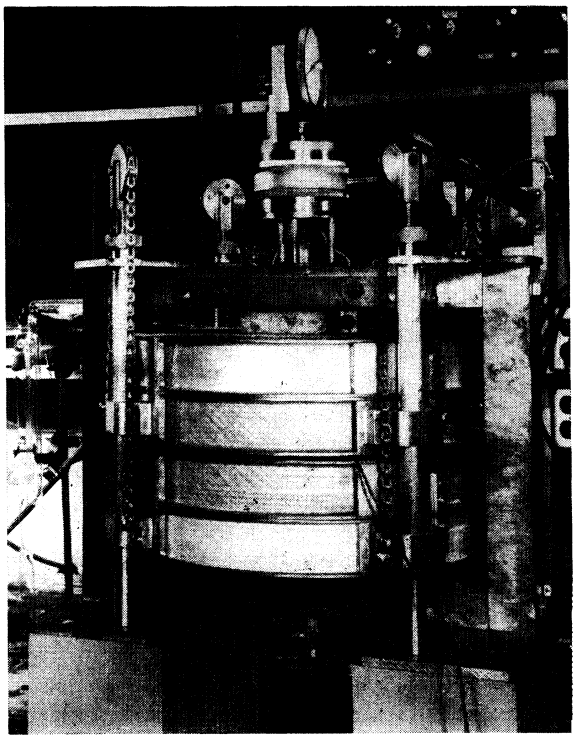

FIG. 3. The microwave cavity spectroscope for measuring Zeeman and Paschen-Back effects.

[4] Kellogg, Rabi, and Ramsey, Jr., Phys. Rev. **57**, 677 (1940).
[5] E. U. Condon and G. H. Shortley, *The Theory of Atomic Spectra* (Cambridge University Press, London, 1935).

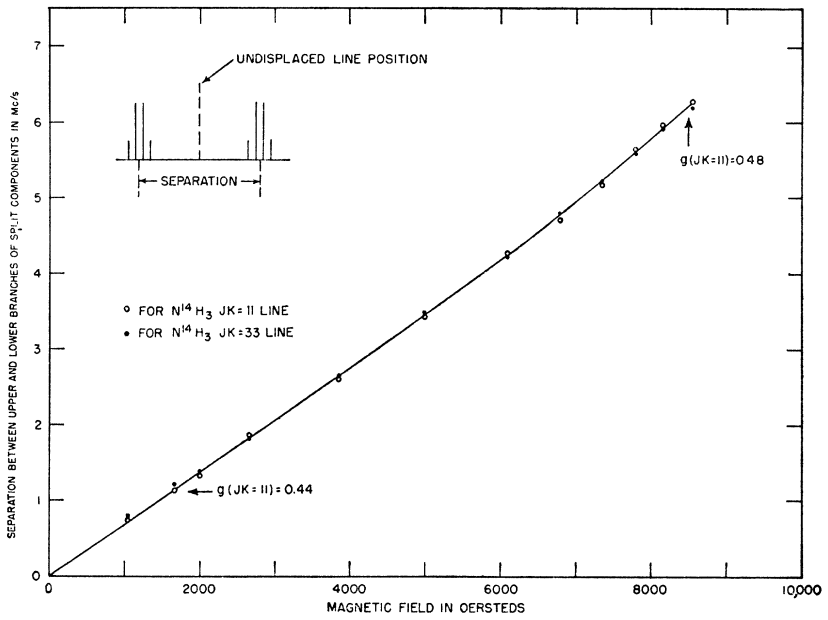

FIG. 4. Zeeman and Paschen-Back splitting for $N^{14}H_3$ lines as a function of the magnetic field.

stants, and β denote $M_{J'}M_{I'}$ with a constant J' not necessarily equal to J, and I' always equal to I. Further, let A and B represent states in an intermediate magnetic field which would go over, respectively, to the states represented by α and β at infinite field. The intensity of transition is known to be proportional to $|(A|\mathbf{P}|B)|^2$, where $\mathbf{P}$=electric moment vector. This matrix element $(A|\mathbf{P}|B)$ is, to the first-order preturbation, as follows:[5,6]

$$(A|\mathbf{P}|B)=(\alpha|\mathbf{P}|\beta)+\sum_{\beta'\neq\beta}\frac{(\alpha|\mathbf{P}|\beta')(\beta'|H_Q|\beta)}{W_0(\beta)-W_0(\beta')}+\sum_{\alpha'\neq\alpha}\frac{(\beta|\mathbf{P}|\alpha')(\alpha'|H_Q|\alpha)}{W_0(\alpha)-W_0(\alpha')},\quad(8)$$

where each W_0 has the following form

$$W_0(\alpha)=W_R(JK\delta)+W_H(M_JM_I)=W_R(JK\delta)-(M_Jg_{\text{mole}}+M_Ig_N)\mu_0H,\quad(8a)$$

which is the unperturbed energy consisting of the rotational energy plus the magnetic energy in an uncoupled state. In addition to the rules given in Eq. (2) for the non-vanishing of the matrix elements of $\mathcal{H}_Q$, the following selection rules for the non-vanishing of the matrix elements of $\mathbf{P}$, such as $(\alpha|\mathbf{P}|\beta)$, are also essential

$$\Delta J=0,\pm1,\quad \Delta M_J=0,\pm1,\quad \Delta M_I=0.\quad(9)$$

If for two states, α and β, the selection rules in Eq. (9) are satisfied, then $(\alpha|\mathbf{P}|\beta)$ in Eq. (8) is finite while the summation terms vanish. The intensity of the transition between A and B is independent of the field strength to this degree of approximation. Such transitions are said to be "allowed" in the decoupled state. On the other hand, if the conditions in Eq. (9) are not satisfied, $(\alpha|\mathbf{P}|\beta)$ would certainly vanish, but the summation terms will not necessarily be zero. Wherever the latter terms contribute something, the transition between A and B would have a finite intensity, in spite of the fact that it is "forbidden" by the selection rules in Eq. (9). Such contributions are, however, necessarily field-dependent, because the denominator in each summation term is seen to be proportional to H from Eq. (8a). The intensity of such "forbidden" lines vary, to this approximation, inversely as the square of magnetic field strength.

The characteristics of a Paschen-Back pattern in intermediate fields, when one nuclear quadrupole coupling is involved, will be illustrated by a concrete example in Section V. However, a few salient features of the general problem can be brought out by treating the case of an almost infinitely high field. Using Eqs. (7) and (9), the following results for the transition frequencies are obtained.

(a) The $J\rightarrow J$ transition frequencies $(H\rightarrow\infty)$ are:

$$\nu_\pi=\nu_R,\quad(10)$$

$$\nu_\sigma{}^{\pm}(M_JM_I)=\nu_R\pm\{g_{\text{mole}}(\mu_0H/h)+(3C/2h)(2M_J+1)[I(I+1)-3M_I{}^2]\},\quad(11)$$

where $M_J\neq J$ and h=Planck's constant. The π-transition is a single line at the rotation frequency ν_R. The σ-transition consists of a fine structure with $2J(I+1)$ components in each branch (+ or −). The two branches of the σ-transitions are symmetrical with respect to ν_R and the components of each branch are symmetrical

[6] For conciseness, a small effect has been neglected resulting from the wave function not being renormalized after perturbation. Actual numerical calculations presented in Section V have, however, taken this into account.

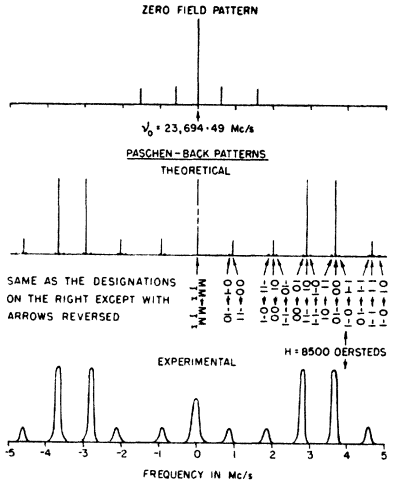

FIG. 5. Theoretical and experimental Paschen-Back patterns for $N^{14}H_3$ $JK=11$ line at $H=8500$ oersteds. (In the middle diagram, each line represents the over-all intensity of a group of transitions whose positions are indicated by the dots.)

with respect to its center of gravity. The effect of the nuclear g-factor is necessarily absent in the decoupled state because $\Delta M_I=0$. The molecular g-factor is related to the σ-transitions, by Eq. (11), as follows:

$$g_{\text{mole}}=\frac{h\{\nu_\sigma^+(M_JM_I)-\nu_\sigma^-(M_JM_I)\}}{2\mu_0 H}, \tag{12}$$

or

$$=\frac{h\{\nu_\sigma^+(\text{c.b.})-\nu_\sigma^-(\text{c.b.})\}}{2\mu_0 H}, \tag{13}$$

where c.b. denotes the center of each branch. The constant C, which is proportional to the quadrupole coupling factor, is related to the fine structure separation, again by Eq. (11), as follows:

$$C=\pm\frac{2h\{\nu_\sigma^\pm(M_J'M_I')-\nu_\sigma^\pm(M_JM_I)\}}{3\{(2M_J'+1)[I(I+1)-3(M_I')^2]-(2M_J+1)[I(I+1)-3M_I^2]\}}. \tag{14}$$

(b) The $J\rightarrow J+1$ transition frequencies ($H\rightarrow\infty$) are:

$$\nu_\pi(M_JM_I)=\nu_R+(1/2h)\{C'[(J+1)(J+2)-3M_J^2]-C[J(J+1)-3M_J^2]\}[I(I+1)-3M_I^2] \tag{15}$$

and

$$\nu_\sigma^\pm(M_JM_I)=\nu_R\pm\left\{g_{\text{mole}}\frac{\mu_0 H}{h}+\frac{3C'}{h}M_J[I(I+1)-3M_I^2]\right\}+(1/2h)\{C'[(J+1)(J+2)-3(M_J^2+1)]-C[J(J+1)-3M_J^2]\}[I(I+1)-3M_I^2], \tag{16}$$

where C' has the same expression as C, with J replaced by $J'=J+1$. It is seen that the π-transition has a fine structure with $(J+1)(I+1)$ components, while each branch of the σ-transition has $(2J+1)(I+1)$ components. One important feature of these transitions is the asymmetric nature of the patterns. The pattern for the π-transition is not symmetrical with respect to ν_R, while the pattern for the σ-transitions is neither symmetrical with respect to ν_R nor with respect to the π-transitions. Expressions similar to Eqs. (12)–(14) can be easily derived for this case also, but they will not be given here.

V. CALCULATIONS FOR $N^{14}H_3$ AND COMPARISON WITH EXPERIMENTAL RESULTS

The solution for the $N^{14}H_3$ eigenvalue problem in intermediate magnetic fields is relatively easy, because the order of the secular equation is cubic [$I(N^{14})=1$]. The determinantal equation is

$$\begin{vmatrix}\mathcal{E}_{11}-E & \mathcal{E}_{12} & \mathcal{E}_{13}\\ \mathcal{E}_{21} & \mathcal{E}_{22}-E & \mathcal{E}_{23}\\ \mathcal{E}_{31} & \mathcal{E}_{32} & \mathcal{E}_{33}-E\end{vmatrix}=0, \tag{17}$$

where

$$\mathcal{E}_{11}=-\{(M+1)g_{\text{mole}}+g_N\}\mu_0 H-(C/2)\{J(J+1)-3(M+1)^2\},$$

$$\mathcal{E}_{22}=-Mg_{\text{mole}}\mu_0 H+C\{J(J+1)-3M^2\},$$

$$\mathcal{E}_{33}=-\{(M-1)g_{\text{mole}}+g_N\}\mu_0 H-(C/2)\{J(J+1)-3(M-1)^2\},$$

$$\mathcal{E}_{12}=\mathcal{E}_{21}=-[3C/(8)^{\frac{1}{2}}](1+2M)[(J+1+M)(J-M)]^{\frac{1}{2}},$$

$$\mathcal{E}_{23}=\mathcal{E}_{32}=-[3C/(8)^{\frac{1}{2}}](1-2M)[(J+1-M)(J+M)]^{\frac{1}{2}},$$

$$\mathcal{E}_{13}=\mathcal{E}_{31}=(3C/2)[\{J+1)^2-M^2\}(J^2-M^2)]^{\frac{1}{2}},$$

and $M=M_J+M_I$, $E=W-W_R(JK\delta)$.

The calculated results for E as a function of the magnetic field are plotted in Fig. 6, using constants previously obtained in (I). For direct comparison with experiment, transition frequencies between the two inversion levels[7] and their intensities according to Eq. (8) are calculated for a constant field of 8500 oersteds and plotted in the center picture of Fig. 5. It is seen that there is generally a good agreement between the theoretical and experimental results.[8] Each strong line in the experimental pattern is now recognized to represent one (or several) of the allowed transitions satisfying Eq. (9). The weak lines, having field-dependent intensities are "forbidden" by the same selection rules. The statement made in Section III, that the weak lines were barely detectable in a field of 10,000 oersteds,

[7] For convenience, transitions are indicated in Fig. 6 between the magnetic levels belonging to one inversion state instead of two magnetic levels, one belonging to each inversion state.

[8] The experimental intensity of the π-line at the center ($\Delta M_J=\Delta M_I=0$) should not be compared on the same basis with those of the σ-lines, because the cavity-mode responses do not give π- and σ-lines the same weight factor.

should mean that the decoupling is not quite complete even in this field.

The agreement between the theory and experiment in the case of the molecular g-factors is also quite satisfactory. Equation (12) or (13), which applies directly to the case of $N^{14}H_3$, states that the g_{mole} can be determined from the frequency separation between the centers of the two branches in the σ-transition at very high fields. The experimental results plotted in Fig. 4 show that the measured g-factor at high fields does approach asymptotically the value previously obtained in (I), $g_{\text{mole}}=0.48$.

The two strong lines in each branch of the experimental pattern for the σ-transition in Fig. 5 are interpreted, in the light of the theory, as two distinct groups of unresolved fine structure lines. The frequency separation between the two groups is, by Eq. (14), a measure of the nuclear quadrupole coupling factor. A determination of the coupling factor from the Paschen-Back pattern gives a result in essential agreement with the value determined from the multiplet structure at zero field.

VI. PASCHEN-BACK EFFECT IN N_2O SPECTRUM

The microwave rotational spectra of N_2O were studied first by Coles, Elyash, and Gorman,[9] later by Smith, Ring, and Gordy,[10] and more recently by Coles and Hughes.[11] The first group of observers determined the rotational frequencies of $N^{14}N^{14}O$ (O for O^{16} throughout this section) and $N^{15}N^{14}O$ and gave values for the nuclear electric quadrupole coupling factors for the end and center N^{14} nuclei. The second group of observers redetermined the quadrupole coupling factor for the end N^{14} nucleus by applying Bardeen and Townes' theory[12] of two-nuclear coupling to their own results. The last group published the frequency measurement of the two other isotopic species, $N^{14}N^{15}O$ and $N^{15}N^{15}O$.

The N_2O molecule is interesting from the standpoint of studying the Paschen-Back effect because, first, its quadrupole interaction is conveniently small, and second, it offers a variety of different quadrupole coupling types ($N^{14}N^{14}O$ for two-nuclear coupling, $N^{15}N^{14}O$ and $N^{14}N^{15}O$ for one-nuclear coupling at different positions, and $N^{15}N^{15}O$ for no coupling). The simplicity of a $J=0\rightarrow1$ transition is another favorable feature.

In this experiment, some detailed studies on the $N^{14}N^{14}O$ spectrum and a brief examination of the effects in $N^{15}N^{14}O$ have been made.[13] In the case of $N^{14}N^{14}O$, the end N^{14} nucleus has a quadrupole coupling factor $(eQ/h)(\partial^2V/\partial z^2)=-1.02$ mc/s[10] (to be compared with the value -4.18 mc/s for N^{14} in $N^{14}H_3$) and the center N^{14} has a factor of -0.27 mc/s.[9] Figure 7 shows the observed triplet structure for $N^{14}N^{14}O$ in zero field.

According to the theory,[12] the two lower-frequency triplet components are expected to have fine structures of their own, provided the resolution is sufficiently high. The theoretical results in zero field are illustrated by the spectrum drawn directly above the experimental pattern. Since one nucleus has a much stronger coupling than the other, the gross triplet structure is essentially due to the stronger coupling, while the fine structure is due to the weaker coupling, which can be regarded as a perturbation.

The effect on the $N^{14}N^{14}O$ spectrum of increasing the magnetic field from zero can be thought of as a Zeeman range at extremely low fields and then another range of gradual decoupling at somewhat higher fields. Although such transition effects have been observed to take place qualitatively, they could not be measured with certainty because of the presence of many components within a frequency range of about one mc/s.

In contrast with the low field phenomena, the Paschen-Back spectrum for $N^{14}N^{14}O$ at fields above $H=5000$ oersteds presented a strikingly simple pattern. There were two stronger σ-lines, one on each side of the center (position of the zero field strongest line), and two π-lines (one strong and one weak) slightly displaced in opposite directions from the center. The line intensities increased with the field strength, but became almost

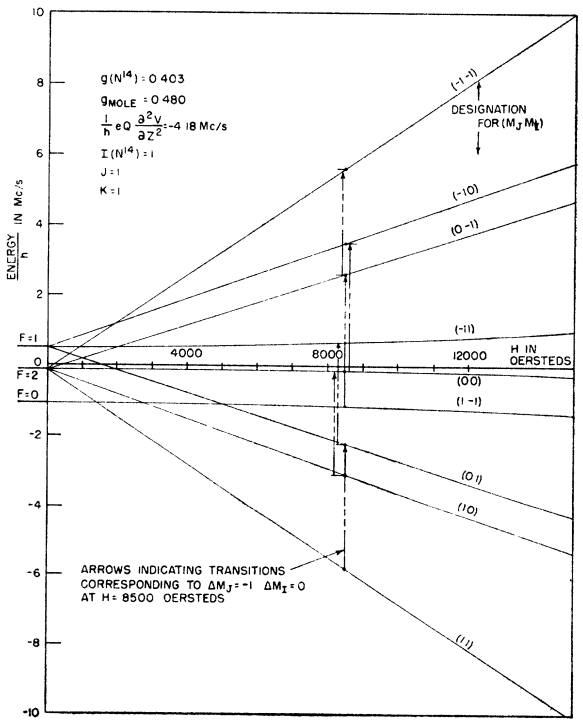

FIG. 6. Energy levels for $N^{14}H_3$ $JK=11$ state as a function of the magnetic field.

[9] Coles, Elyash, and Gorman, Phys. Rev. **72**, 973 (1947).
[10] Smith, Ring, and Gordy, Phys. Rev. **73**, 633 (1948).
[11] D. K. Coles and R. H. Hughes, Phys. Rev. **76**, 178 (1949).
[12] J. Bardeen and C. H. Townes, Phys. Rev. **73**, 97 (1948).
[13] The author is indebted to Professor E. B. Wilson, Jr. and Dr. D. K. Coles for generously supplying samples for this experiment.

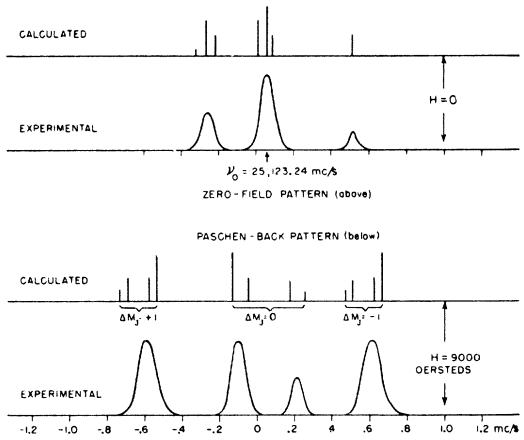

FIG. 7. Theoretical and experimental zero-field and Paschen-Back patterns for $N^{14}N^{14}O$ $J=0\rightarrow1$ rotational transition.

field-independent beyond $H=8000$ oersteds. The pattern at $H=9000$ oersteds is shown in the lower picture of Fig. 7. Use of still higher fields did not result in any noticeable change in the pattern.

The Paschen-Back effect in the $N^{15}N^{14}O$ spectrum at strong fields was found to be essentially the same as in the $N^{14}N^{14}O$ spectrum except that the line intensities reached their steady values at a lower field and that the π-line apparently remained single and was not appreciably displaced from the center.

VII. INTERPRETATION OF THE N_2O PASCHEN-BACK SPECTRUM

The experimental results described in the preceding section can be evaluated in terms of a simplified theory. It will be assumed that the magnetic field is large enough to decouple the nuclear spins from the molecular rotation. In the JIM_JM_I representation, the matrix for the total Hamiltonian is sensibly diagonal at very high fields. The eigenvalues can be directly written as[14]

$$W=W_0-\{M_Jg_{\text{mole}}+(M_{I1}+M_{I2})g_N\}\mu_0H$$
$$+(C_1/2)[J(J+1)-3M_J^2][I_1(I_1+1)-3M_{I1}^2]$$
$$+(C_2/2)[J(J+1)-3M_J^2][I_2(I_2+1)-3M_{I2}^2], \quad (18)$$

where all quantities have the same meaning as in Eq. (1) except for the subscipts 1 and 2 pertaining to the nuclei 1 and 2, each of which has a quadrupole coupling. The selection rules are also exactly the same as in Eq. (9), except that $\Delta M_I=0$ means here $\Delta M_{I1}=0$ and $\Delta M_{I2}=0$.

For the N_2O spectrum, $I_1=I_2=1$, $J=0$ for the ground state, and $J=1$ for the upper state, the energy expressions are even more simplified. It is readily shown that the $\pi(\Delta M_J=0)$ and $\sigma(\Delta M_J=\pm1)$ transitions are:

$$\pi\text{-lines:}\quad \nu_\pi(M_{I1}M_{I2})=\nu_R+(C_1/h)(2-3M_{I1}^2)$$
$$+(C_2/h)(2-3M_{I2}^2), \quad (19)$$

$$\sigma\text{-lines:}\quad \nu_\sigma^{\pm}(M_{I1}M_{I2})=\nu_R\pm g_{\text{mole}}\mu_0H/h$$
$$-(C_1/2h)(2-3M_{I1}^2)-(C_2/2h)(2-3M_{I2}^2), \quad (20)$$

where each C is the value of C (Eq. (1)) at $J=1$. The molecular g-factor (g_{mole}) and the quadrupole coupling parameters (C_1 and C_2) can be directly derived from Eqs. (19) and (20) with the following results:

$$g_{\text{mole}}=\frac{h\{\nu_\sigma^+(M_{I1}M_{I2})-\nu_\sigma^-(M_{I1}M_{I2})\}}{2\mu_0H}, \quad (21)$$

$$C_1=(h/3)\{\nu_\pi(0\pm1)-\nu_\pi(\pm1\pm1)\}, \quad (22)$$

$$C_2=(h/3)\{\nu_\pi(\pm10)-\nu_\pi(\pm1\pm1)\}. \quad (23)$$

It is noted from Eqs. (19) and (20) that both the π- and σ-lines in the Paschen-Back spectrum for the case of two-nuclear coupling have fine structures, resulting from the nuclear quadrupole interactions. The σ-lines are, for the $J=0\rightarrow1$ transition, asymmetrical relative to the π-lines because of non-linear dependence of the interaction energy upon M_J and M_I. Equation (21) states that the molecular g-factor can be deduced from the frequency separation between any σ-line and its "image," if the lines are resolved, or between "+" and "−" unresolved groups of lines. Equations (22) and (23) show that each quadrupole interaction factor can be determined directly from the fine structure, if there is sufficient resolution for the lines whose separation is caused by that interaction.

A comparison between theory and experiment can now be made. Again in Fig. 7, a theoretical spectrum is drawn directly above the experimental pattern for $H=9000$ oersteds, using the coupling factors cited in Section VI. The approximate agreement between theory and experiment indicates that the spin-rotation decoupling is almost complete for the field used. Since the fine structure of the σ-lines is not experimentally resolved and that of the π-line is only partially resolved, only the larger of the two coupling factors can be experimentally determined. This yields a result which is in essential agreement with the value assumed.

The experimental determination of g_{mole} can be obtained quite accurately, because, in contrast to the determination of the coupling factor, this does not depend upon the resolution of the fine structure. Further, a similar determination has been made from the Paschen-Back spectra for $N^{15}N^{14}O$, for which Eq. (21) would also apply by preserving the contributions of only one nucleus. The results of such determinations for g_{mole} in nuclear units are:

$N^{14}N^{14}O$ $\quad g_{\text{mole}}=0.087\pm0.004$

and

$N^{15}N^{14}O$ $\quad =0.085\pm0.004$.

[14] H. M. Foley, Phys. Rev. **71**, 747 (1947).

Thus, the molecular g-factors for $N^{14}N^{14}O$ and for $N^{15}N^{14}O$ are essentially equal within the limits of experimental error.

VIII. CONCLUSION

The Paschen-Back effect for NH_3 and N_2O molecules has been shown to exist in the microwave spectra with only moderately strong magnetic fields. For both one- and two-nuclear couplings, the experimental results can be satisfactorily interpreted in terms of the quantum mechanical theory of perturbations.

The Paschen-Back effect in the microwave molecular spectra should prove to be useful in interpreting the nature of the spin-rotation coupling and in the direct determination of molecular g-factors.

PHYSICAL REVIEW VOLUME 76, NUMBER 10 NOVEMBER 15, 1949

Impulse Breakdown in the 10^{-9}-Sec. Range of Air at Atmospheric Pressure*,**

R. C. FLETCHER***
Laboratory for Insulation Research, Massachusetts Institute of Technology, Cambridge, Massachusetts
(Received August 1, 1949)

The formative lag of spark breakdown has been measured over the range from 0.5 to 50×10^{-9} sec. using transmission line circuits in conjunction with the micro-oscillograph. It is found to be a function only of the applied field (independent of gap-width) for the shorter times (high fields), but to increase for decreasing gap-widths for the longer times (low fields). A calculation of the formative lag is presented which is based on the assumption that it consists mainly of the time for a single electron avalanche to build up a space-charge field comparable with the applied field. This predicts the observed formative lags within the experimental accuracy of the measurements over the entire range used. The increasing times for decreasing gap-widths for the longer times is interpreted as the transition from a single avalanche to a multiple avalanche mechanism of breakdown. The critical field where this transition takes place for a given gap-width is computed and found to predict the observed critical fields within the experimental accuracy. The good agreement between theory and experiment enables a more reliable prediction than has previously been possible of the critical gap-width above which the threshold field is determined by a single avalanche mechanism.

A sharp drop in the rate of fall of the breakdown voltage is observed for the shorter times. It is suggested that this may be a change in the mechanism of electron release from the cathode.

I. INTRODUCTION

MANY experiments have been performed to measure the formative lag time of the atmospheric spark as a function of applied voltage.[1] Unfortunately this time is so short for a slight overvoltage that oscillograph measurements have previously been impossible, and other indirect schemes have had to be used. These, although often ingenious, have still limited the measurement of the formative lag to a rather small region of applied voltage (i.e., up to about 70 percent overvoltage), where the time varies extremely rapidly with the applied voltage. However, although individual measurements of the formative lag have differed from each other by as much as a factor of five, its order of magnitude and the general shape of its variation with overvoltage have been well established. In fact, the discovery that the order of magnitude of the formative lags was so short led to the suggestion that the Townsend theory had to be either modified or rejected in explaining the breakdown of atmospheric air.[2]

Proposed theories of the atmospheric spark have attempted to predict the observed threshold field and order of magnitude of the formative time.[2,3] Largely because accurate measurements of the formative time were not available, little attempt has been made to compare quantitatively the experimental and theoretical variation of the formative time with applied voltage. Raether has made the suggestion[4] that most of the formative lag consists of the time a single electron avalanche takes to build up to the magnitude where its space-charge field is comparable with the applied field. This suggestion was based on the "streamer" mechanism of breakdown, in which secondary avalanches, initiated before and behind the head of the initial avalanche by photon absorption, build up more rapidly in the enhanced field caused by the space charge. This creates two streamers of ionization which appear to move from the head of the initial avalanche towards the anode and the cathode at a much higher velocity than the velocity of the initial avalanche. Thus the complete spark channel should be established very soon after the space-charge field of the initial avalanche becomes of the order of the applied field. Raether showed that this suggestion explains the general shape

* Sponsored by the ONR, the Army Signal Corps, and the Air Force under ONR Contract N5ori-07801.

** From a doctorate thesis in physics, Massachusetts Institute of Technology.

*** National Research Council Predoctoral Fellow.

[1] A summary is given by R. Strigel, *Elektrische Stossfestigkeit* (Verlag. Julius Springer, Berlin, 1939), p. 34.

[2] J. Slepian, Elec. World **91**, 761 (1928); J. Franck and A. von Hippel, Zeits. f. Physik **57**, 696 (1929); L. B. Loeb, Science **69**, 509 (1929).

[3] L. B. Loeb and J. M. Meek, *The Mechanism of the Electric Spark* (Stanford University Press, Stanford University, California, 1941); H. Raether, Zeits. f. Physik **112**, 464 (1939).

[4] H. Raether, Elektrotech. Zeits. **63**, 301 (1942).

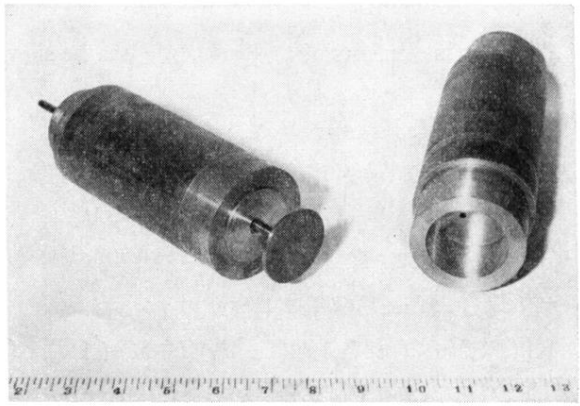

FIG. 1. The microwave cavity and the magnet pole pieces (unassembled view).

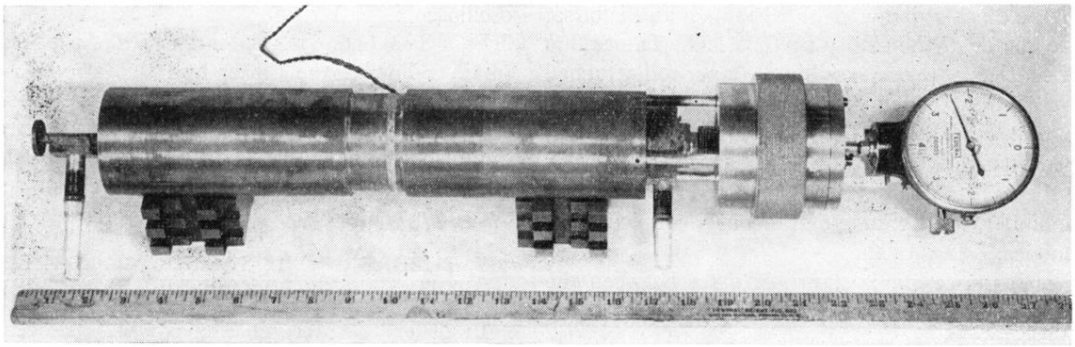

FIG. 2. The microwave cavity and the magnet pole pieces (assembled view).

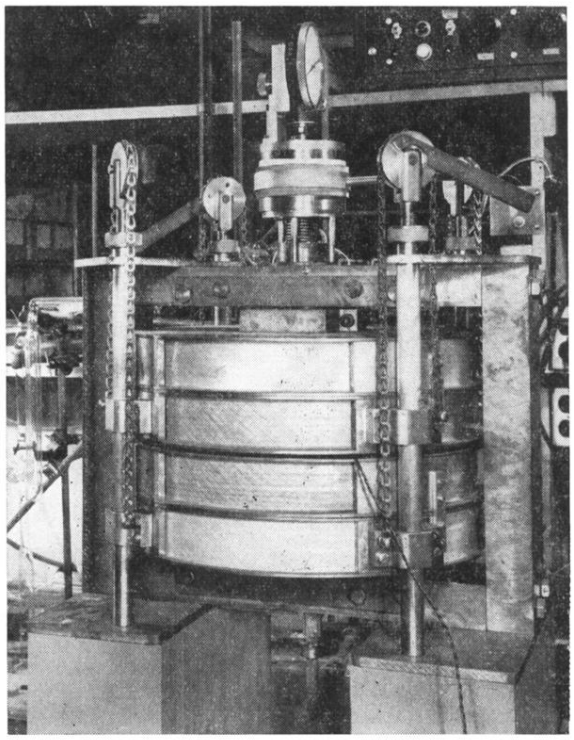

FIG. 3. The microwave cavity spectroscope for measuring Zeeman and Paschen-Back effects.